

# Application of Artificial Neural Networks to Rainfall Forecasting in Queensland, Australia

John ABBOT\* and Jennifer MAROHASY

*Centre for Plant and Water Science, Central Queensland University, Bruce Highway,*

*Rockhampton Q. 4702, Australia*

(Received 9 December 2011; revised 23 January 2012)

## ABSTRACT

In this study, the application of artificial intelligence to monthly and seasonal rainfall forecasting in Queensland, Australia, was assessed by inputting recognized climate indices, monthly historical rainfall data, and atmospheric temperatures into a prototype stand-alone, dynamic, recurrent, time-delay, artificial neural network. Outputs, as monthly rainfall forecasts 3 months in advance for the period 1993 to 2009, were compared with observed rainfall data using time-series plots, root mean squared error (RMSE), and Pearson correlation coefficients. A comparison of RMSE values with forecasts generated by the Australian Bureau of Meteorology's Predictive Ocean Atmosphere Model for Australia (POAMA)-1.5 general circulation model (GCM) indicated that the prototype achieved a lower RMSE for 16 of the 17 sites compared. The application of artificial neural networks to rainfall forecasting was reviewed. The prototype design is considered preliminary, with potential for significant improvement such as inclusion of output from GCMs and experimentation with other input attributes.

**Key words:** general circulation models, artificial neural networks, rainfall, forecast

**Citation:** Abbot, J., and J. Marohasy, 2012: Application of artificial neural networks to rainfall forecasting in Queensland, Australia. *Adv. Atmos. Sci.*, **29**(4), 717–730, doi: 10.1007/s00376-012-1259-9.

---

## 1. Introduction

### 1.1 *Limitation of traditional models for rainfall forecast*

Understanding the complex physical processes that create rainfall remains a major challenge, and accurate rainfall forecasting remains an important ideal, with significant implications for food production, securing water supplies for major population centers, and minimizing flood risks. Three-quarters of the state of Queensland, Australia, was declared a disaster zone following torrential rains during the summer of 2010–2011 (Hurst, 2011). Official weather and climate forecasts failed to predict the magnitude of the event, creating particular issues for dam management, which resulted in abrupt water releases that contributed to the flooding of the capital city, Brisbane (Seqwater, 2011; Queensland Flood Commission of Inquiry, 2011).

The Australian Bureau of Meteorology (BOM) produces seasonal rainfall outlooks and regular updates

on ENSO, and it is working to improve seasonal and intraseasonal rainfall forecasts using the Predictive Ocean Atmosphere Model for Australia (POAMA), a GCM under development for 10 years (Zhao and Hendon, 2009; Hudson et al., 2011). The Queensland Department of Environment and Resource Management also produces a seasonal rainfall forecast known as SPOTA-1 (Seasonal Pacific Ocean Temperature Analysis), based on statistical analyses of climate indices (Day et al., 2010).

### 1.2 *Introducing artificial neural networks*

Artificial neural networks are not currently used in Australia for official rainfall forecasts, and there has been limited consideration of their possible application beyond short-term forecasting of rainfall in the Parramatta catchment (Luk et al., 2000; Luk et al., 2001; Nasser et al., 2008). In other parts of the world, particularly Asia, the use of artificial neural networks for short-, medium-, and long-term forecasting is an active area of research within the meteorology and mathe-

---

\*Corresponding author: John ABBOT, j.abbot@cqu.edu.au

matics and computing communities (e.g., French et al., 1992; Tangang et al., 1998; Chattopadhyay and Chattopadhyay, 2008).

Extensive literature is available on the theoretical principles behind neural networks and their applications in a wide range of disciplines including science, engineering, and economics. The mathematical fundamentals of neural networks and specific applications in hydrology, including rainfall, have been reviewed in a two-part series (ASCE Task Committee on Application of Artificial Neural Networks in Hydrology, 2000a, b). Artificial neural networks are massive, parallel-distributed, information-processing systems with characteristics resembling the biological neural networks of the human brain. Typically, an artificial neural network is configured with the following characteristics: (1) information processing occurs at many single elements called nodes, or neurons; (2) signals are passed between nodes through connection links; (3) each connection link has an associated weight that represents its connection strength; and (4) each node typically applies a nonlinear transformation called an activation function to its net input to determine its output signal.

Most applications in rainfall forecasting utilize a feed-forward neural network that incorporates the standard static multilayer perceptron (MLP) trained with the back-propagation algorithm (e.g., Karamouz et al., 2008). This configuration provides a static network, lacking a memory capability. The MLP model does not incorporate temporal processing, and the input vector space does not consider temporal relationships among inputs (Giles et al., 1997) often leading to suboptimal solutions. There are various ways that a “memory” capability can be introduced into static neural networks, making them dynamic. In increasing order of complexity and capability, dynamic models include the following:

(1) Tapped delay line models: The network has past inputs explicitly available through a tapped delay line (Mozer and Smolensky, 1989). The use of these internal time-delay operators enables the network to behave dynamically and leads to the conventional time-delay neural network (TDNN).

(2) Context or partial recurrent models: The network retains the past output of nodes instead of retaining the past raw inputs; for example, the output of the hidden layer neurons of a feed-forward network can be used as inputs to the network along with the true inputs (Elman, 1990).

(3) Fully recurrent models: The network employs full feedback and interconnections between all nodes. Algorithms to train fully recurrent models are significantly more complex in terms of time and storage re-

quirements (Pineda, 1989).

Once feedback connections are included as in items (2) and (3), a neural network becomes a recurrent neural network (RNN). The features of RNN and TDNN can be combined leading to an extended dynamic neural network known as a time-delay RNN (TDRNN).

The model that we developed to forecast rainfall in Queensland is a dynamic stand-alone recurrent, time-delay neural network—a TDRNN.

### 1.3 Types of neural network rainfall models

There are at least three approaches to modeling that can be used in combination with artificial neural networks.

#### 1.3.1 Function models

Most forecasting of rainfall with artificial neural networks has been done with what are known as static function models. These models use sets of attribute values as input with the goal of predicting a corresponding forecast rainfall value. Each input set of attribute values may comprise lagged rainfall values, or other lagged climate-related values, for example, the Southern Oscillation Index (SOI) or a combination of both.

Wu et al. (2001) generated forecasts for monsoon rainfall in China up to 10 years in advance using only historical rainfall data as input. Philip and Joseph (2003) forecast monthly rainfall for Kerala State in the southern part of the Indian Peninsula with only historical monthly rainfall data. Chakraverty and Gupta (2008) input only rainfall data to predict Indian monsoon rainfall 6 years in advance. Chattopadhyay and Chattopadhyay (2008) relied on 129 years of historical rainfall data (1871 to 1999) to forecast annual summer-monsoon rainfall over India with a 1-year lead time. Other examples include Bilgili and Sahin (2010) forecasting monthly rainfall for stations in Turkey, Gholizadeh and Darand (2009) forecasting 1 year in advance for Tehran in Iran, and Freiwan and Cigizoglu (2005) forecasting 1 month in advance for Amman airport in Jordan.

Other investigators have used sets of climatic values as input with a function modeling approach, without rainfall itself as input (e.g., Navone and Ceccatto, 1994). Silverman and Dracup (2000) used a static function neural network to forecast the total annual precipitation for California’s seven climatic zones using input data from climatic indices including the SOI. Hartman et al. (2008) used a set of climatic indices again including SOI and also SSTs to forecast summer rainfall in the Yangtze River Basin in China. Venkatesan et al. (1997) used a set of 10 input parameters, including sea level pressures and SSTs to forecast an-

nual Indian monsoon rainfall. Iseri et al. (2005) used a combination of various lagged climate indices, including the SOI and Pacific Decadal Oscillation (PDO) as well as SSTs, to forecast monthly rainfall three months in advance for the city of Fukuoka in Japan. Forecasts of Indian monsoon rainfall have been made 10 months in advance using a static function model with 10 input parameters, including temperatures and pressures (Guhathakurta et al., 1999).

There have been relatively few investigations where static function models have used a combination of historical rainfall data and other climatic attributes. Kulshretha and George (2007) forecast annual rainfall in India with rainfall and monthly temperatures as input. Long et al. (1997) forecast seasonal rainfall from historic rainfall data in combination with other attributes in China.

### 1.3.2 Classification models

Classification models have been used in Australia to forecast rainfall independently of artificial neural networks. Firth et al. (2005) used a nonlinear classification system to predict the onset of Australian winter rainfall. Day et al. (2010) used a classification model that incorporates SOI as the basis of their official forecast for Queensland's grazing region. Micevski et al. (2006) used a classification model based on the Interdecadal Pacific Oscillation (IPO) to describe long-term variability in eastern Australian flood data.

Classification trees attempt to assign attributes to predetermined classes through a process of hierarchical data partitioning. The objective is to produce a tree-based classifier that will enable assignment of any newly observed individual to its correct class with high probability.

Although artificial neural networks are commonly applied to the general problem of classification, there has been limited application of neural networks in combination with classification models to forecast rainfall (Castellani et al., 1996)). Michaelides et al. (2001) use a neural network to group similar patterns belonging to the same classes to describe the temporal distribution of rainfall in Cyprus over the period 1917–1995, but they do not actually forecast rainfall. To achieve a detailed analysis and the trained neural network models capable of differentiating between the various classes, an optimum of 16 classes of rainfall were used.

### 1.3.3 Time series models

Time series neural network models output rainfall values over series of discrete intervals of time.

Htike and Khalifa (2010) used a TDNN to forecast rainfall for Subang in Malaysia between 1980 and 2009 with historical rainfall values as the sole input. Kar-

mamouz et al. (2008) use both TDNNs and TDRNNs with a combination of large-scale climate signals, such as sea-surface pressure and rainfall, to forecast seasonal rainfall in Iran with a 6-month lead time.

Of the published studies we reviewed, our model is most similar in terms of neural network configuration to the model used by Karmamouz et al. (2008).

It is difficult to compare and contrast the different types of models to evaluate their skill at rainfall forecasting because researchers generally provide only a comparison of their output with observed values for the different regions and time periods.

## 2. Data

Dynamic artificial neural networks depend on a set of input predictor data. The datasets need to describe relevant attributes, to be of high quality, and to span comparable periods of time, with longer data series generally preferable to shorter series. In the development of our neural network for Queensland rainfall, we divided the attributes into four classes: (a) monthly rainfall, (b) climatic indices, (c) atmospheric temperatures, and (d) solar data. However, we recognize other potential attributes that could be input, for example, changes in atmospheric carbon dioxide, cosmic ray galactic flux (Erykin et al., 2009; Laken et al., 2010; Kirkby et al., 2011), and lunar tides (e.g., Vines, 2008).

Neural networks are applied by first using a portion of each data set to “train” the network. Another, usually smaller, subset of the data is set aside to validate the reliability of the trained network. In the development of our model we divided the rainfall data for each site so that 85% was used for training corresponding to the period from January 1900 to June 1993 (1122 samples or 93.5 years), and 15% for validation corresponding to the period from July 1993 to December 2009 (198 samples or 16.5 years).

### 2.1 Monthly rainfall

Monthly rainfall data from the Australian Bureau of Meteorology's High Quality Climate Database was input for 20 sites in Queensland (Fig. 1). The sites were chosen on the basis of quality of data, that is, long series with few missing values. All sites selected have between zero and four missing values over the entire range, with the exception of Cheriton. The mean of the values on either side was substituted for each missing value, with the exception of Cheriton which had a longer period of missing values with the corresponding values taken from the nearest high-quality site at Surat.

Many of the sites were within a region defined by

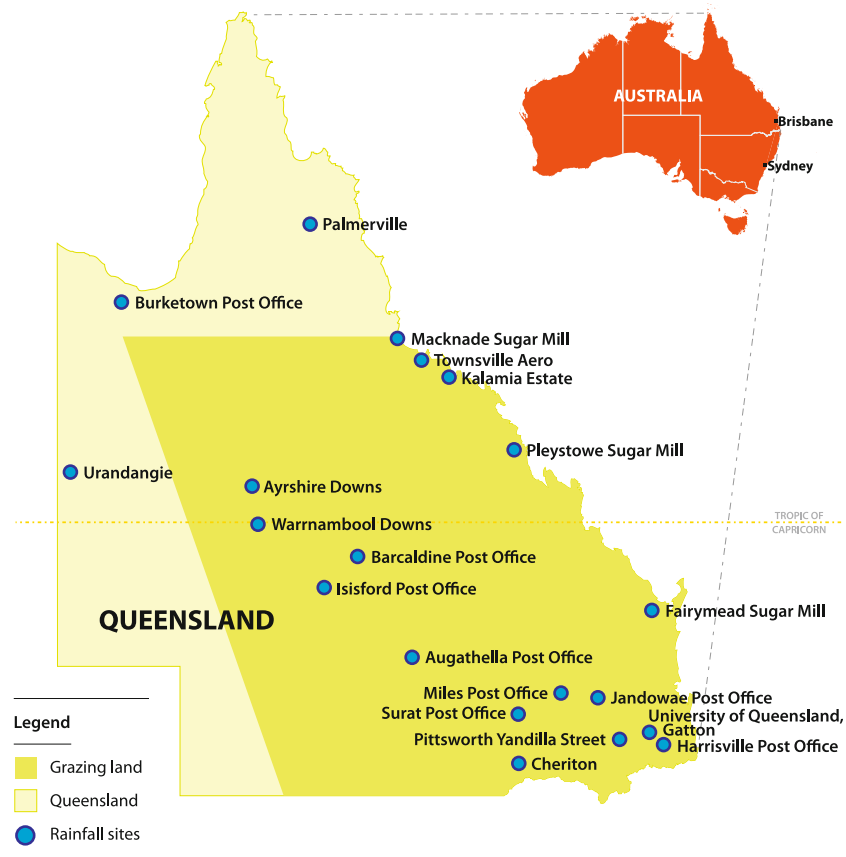


Fig. 1. Map of Queensland with high-quality rainfall sites.

the Queensland government as “the major grazing region” (Day et al., 2010). The Queensland government provides a specific seasonal forecast for this region (Fig. 1).

The total input dataset for each location comprised the complete monthly rainfall record from January 1900 to December 2009, with 1320 samples for each site. In addition we used a set of monthly rainfall data, lagged up to 12 months.

## 2.2 Climate indices

Intraseasonal, interannual, and decadal variability in Queensland rainfall has been linked to complex physical phenomena remote to the Australian land mass (Risbey et al., 2009; Kirono et al., 2010). The phenomena are apparent as recurring patterns in SST and air pressure described numerically by climate indices. The dominant phenomenon is the ENSO that spans the Pacific Ocean. ENSO has two phases, La Niña and El Niño, with El Niño events associated with below-average rainfall often resulting in extended periods of drought over much of northern and eastern Australia (McBride and Nicholls, 1983; Power et al.,

1999; Power et al., 2006).

The SOI is a quantitative estimate of ENSO used extensively in long-range forecasting of rainfall in Australia (e.g., Nicholls et al., 1996; Suppiah, 2004; Meinke and Stone, 2005; Braganza et al., 2009). SOI is defined as the normalized atmospheric pressure difference between Tahiti and Darwin, and we used SOI values calculated by the Climate Research Unit, University of East Anglia. We also used Niño 3.4 to describe ENSO. Niño 3.4 is a measure of SST difference with data compiled by the Hadley Centre, UK Met Office for particular latitudes and longitudes normalized to the period 1971–2000.

There is some evidence that the relationship between ENSO and rainfall is modulated by phases of the Interdecadal Pacific Oscillation (IPO) (e.g., Power et al., 2006). When the IPO is in a negative phase, the impact of ENSO on Queensland rainfall is enhanced (e.g., Verdon and Franks, 2006). The IPO index is compiled infrequently, so we used the related PDO index of Nate Mantua compiled by the University of Washington based on HadSST (1900–1980), OI SST v1 (1982–2001), and OI SST v2 (2002–present).

Phenomena in the tropical Indian Ocean can also influence Queensland rainfall; the Indian Ocean Dipole (IOD) has been found to have some influence particularly in spring (Risby et al., 2009). Some researchers argue that Indian Ocean variability has a larger influence than ENSO on the incidence of drought in Australia (e.g., Ummerhofer et al., 2009).

The Dipole Mode Index (DMI) is a measure of the IOD defined as the difference in SST between the tropical western Indian Ocean and the tropical southeastern Indian Ocean. We used the DMI based on HadISST1 (1870–present).

All of the data series for the indices we used are available as monthly values from 1900 to 2009 at the Royal Netherlands Meteorological Institute (KNMI) Climate Explorer—a web application that is part of the World Meteorological Organisation and European Climate Assessment and Dataset project (2011)<sup>a</sup>. We input current and lagged monthly values.

We recognize that ENSO and the IOD can be described by other indices and that there are many other phenomena, including the Madden-Julian Oscillation (MJO) (Rashid et al., 2011) and the Southern Annular Mode (SAM) (Marshall et al., 2011) that have been shown to impact Queensland rainfall. One limitation of these indices is that they do not extend back to 1900.

We hope to consider other phenomena and more indices in future research.

### 2.3 Atmospheric temperatures

The longest high-quality atmospheric temperature data series for eastern Australia is for Observatory Hill, Sydney, with maximum and minimum temperature records dating to 1859. We used these data, available from the Australian Bureau of Meteorology, as input. There is no comparable temperature dataset available for any Queensland location.

### 2.4 Solar data

Climate indices, rainfall, and temperature can be regarded as internal features of the climate system. However, variations in rainfall have also been directly associated with variations in a number of external attributes, including solar activity (Thresher, 2002; Tomasino et al., 2004; Versteegh, 2005).

We used sunspot numbers and total solar irradiance as inputs because long series of high-quality data are available. Monthly measured total solar irradiance is from Frohlich (2000) with the data downloaded from KNMI Climate Explorer. Sunspot number data was acquired from the Solar Influences Data Analysis

Centre (SIDC) at the Royal Observatory of Belgium, downloaded from KNMI Climate Explorer.

## 3. Method

The neural network software used in this study was Synapse (Peltarion, Stockholm, Sweden). This software provides a versatile neural network platform in which components can easily be combined and tested for many different network topologies. A network was assembled from the set of basic Synapse components, which included the function layer, the weight layer, the gamma memory, as well as standard components for data input and analysis of output. With Synapse, neural networks was also assembled using “snippets,” which are modules preassembled from common combinations of the basic components.

In this study, supervised training was applied by providing the network with the desired output target rainfall (ASCE Task Committee on Application of Artificial Neural Networks in Hydrology, 2000a). During training, the weights of the neurons are modified to achieve a prediction of the next point in the input data. By repeating this procedure with a large input data set (the training set), the neural network “learns” the relationship between input and output data (Chakraverty and Gupta, 2008). The weights are continuously incrementally adjusted, based on the calculated error, which is the difference between ANN output and the target response.

However, there is the potential danger of overtraining a neural network when the network parameters are overly fine-tuned to the training data set. At this point, the network attempts to fit the noise component of the data, as well as learning the more generalized inherent relationships. As a result, the network can perform very well over the dataset used for training, but it may exhibit poor predictive capabilities when presented with new data (Wang and Sheng, 2010).

To prevent overtraining, a cross-training procedure is usually applied, with a portion of the available data reserved for this purpose. Initially, errors for both the training and cross-training datasets decrease. After an optimal amount of training, the errors for the training set continue to decrease, but those associated with the cross-training dataset increase. Further training will likely produce overfitting, and the current set of weights are assumed to be optimal. Synapse enables continuous monitoring of the errors in both the training set and the validation set during training, and this was the approach used in this study to avoid overtraining.

Artificial neural networks can find existing complex

<sup>a</sup> Available at <http://climexp.knmi.nl/about.cgi?id=someone@somewhere>

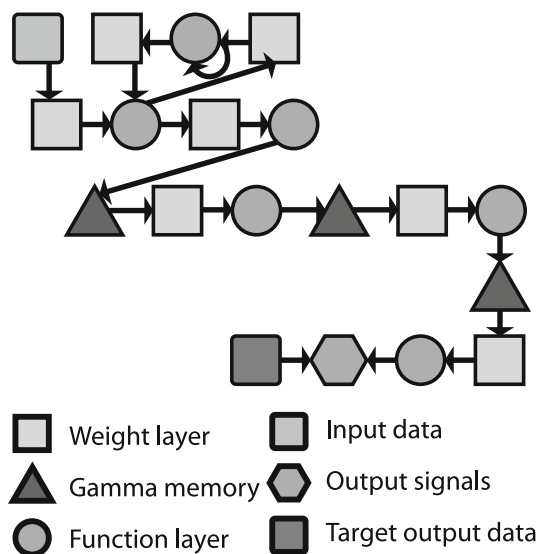


**Fig. 2.** Configuration of the neural network used in this study. The components used were assembled using Synapse (Peltarion).

relationships and patterns repeated over diverse time periods. They can be optimized without a priori knowledge of the underlying physical processes, and they need not be constrained by a priori solution structures (Silverman and Dracup, 2000). One practical limitation may be the amount of time it takes to train the network; training time increases with the size and number of input predictor datasets.

In developing this prototype model it was not possible to predetermine the optimal design of the neural network for any particular combination of inputs. We used trial and error to evaluate different configurations of a dynamic design with the Synapse program. In particular, we decided on a network design which consistently yielded stable error minima for the training and validation sets within 10 000 epochs.

The configuration of the ANN used (Fig. 2), consists of two Synapse snippets connected in series—an Elman network and a TDNN with two hidden layers. This design was then maintained for all evaluations in this study, henceforth referred to as the prototype or the neural network. Although this configuration was maintained throughout the investigation, the network was independently trained for each set of input data. Thus the specific network parameters associated with components differed for each optimization.

Each input data file comprised a matrix of 1320 rows of monthly data commencing January 1900 and up to 33 columns of attributes (Table 1). The output data file comprised a column of forecast monthly rain-

fall corresponding to a 3-month lead from each month defined in the input file.

Our objective was the best possible rainfall forecast corresponding to 3 months in advance measured by the root mean square error (RMSE). For practical reasons, we began with a single site in Queensland, Kalamia Estate, and progressively added the four classes of data (Table 1). Kalamia Estate, which is very approximately halfway along the Queensland east coast, was chosen at random from 20 high-quality rainfall sites (Fig. 1).

Rainfall at Kalamia correlated poorly with each of the input dataset predictors (Pearson correlation coefficient  $< 0.5$ ). This is consistent with the literature of Risbey et al. (2009), which indicates that in most

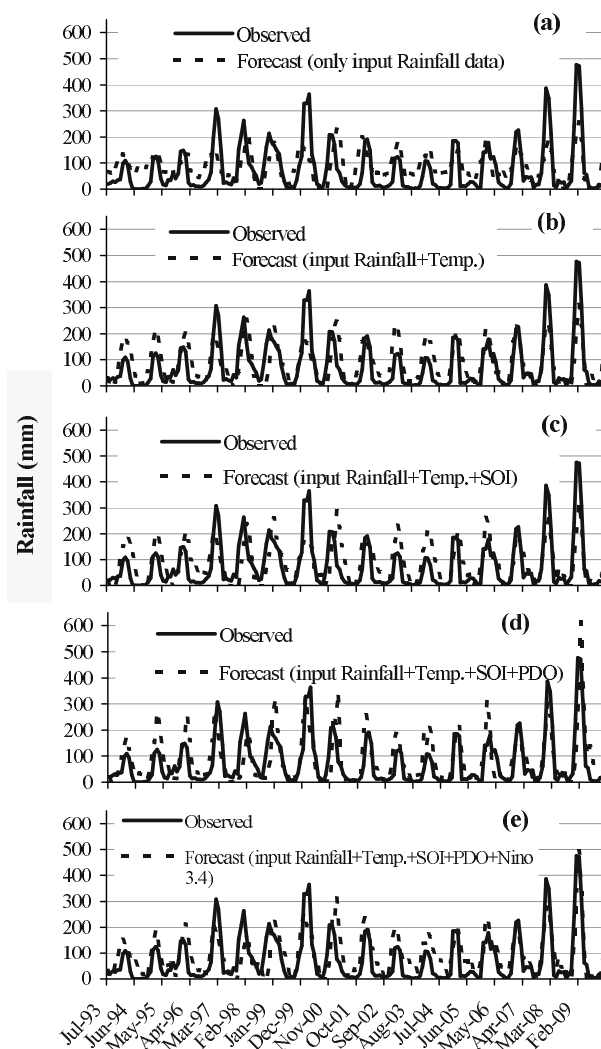


**Fig. 3.** Forecast monthly rainfall (mm) for Kalamia Estate with increasing number of input attributes. The 3-month lead is compared to observed 3-month moving average.

**Table 1.** The four classes of data used to forecast Queensland rainfall. SOI, PDO, Niño 3.4 and DMI are climatic indices that can be downloaded from the Royal Netherlands Meteorological Institute Climate Explorer.

1. Monthly Rainfall (mm)	2. Climate indices	3. Atmospheric Temperature (°)	4. Solar
Current month	SOI current month	Sydney maximum for current month	Sunspot number current month
Lagged 1	SOI lagged 1 month	Sydney minimum for current month	Sunspot number lagged 1 month
Lagged 2	SOI lagged 2 months		Sunspot number lagged 2 months
Lagged 3	PDO current month		Total solar irradiance 1 month
Lagged 4	PDO lagged 1 month		Total solar irradiance lagged 1 month
Lagged 5	Niño-3.4 current month		Total solar irradiance lagged 2 months
Lagged 6	Niño-3.4 lagged 1 month		
Lagged 7	Niño-3.4 lagged 2 months		
Lagged 8	DMI current month		
Lagged 9	DMI lagged 1 month		
Lagged 10	DMI lagged 2 months		
Lagged 11	SOI×PDO month		
Lagged 12			

**Table 2.** Neural network forecast skill relative to input data. The error values, RMSEs, and Pearson correlation coefficients are used to compare the forecast monthly rainfall with 3-month lead forecasts for Kalamia Estate, compared to the 3-month observed moving average.

Inputs	RMSE (mm month <sup>-1</sup> )	Pearson
Current rainfall	76.3	0.60
Current and lagged rainfall	72.0	0.64
Total rainfall + temperatures	66.8	0.69
Total rainfall + temperatures + SOI	73.1	0.65
Total rainfall + temperatures + SOI + PDO	66.6	0.75
Total rainfall + temperatures + SOI + PDO + Solar	71.7	0.65
Total rainfall + temperatures + SOI + PDO + Niño-3.4	62.4	0.77
Total rainfall + temperatures + SOI + PDO + DMI	70.0	0.75

regions the individual drivers of rainfall account for <20% of monthly rainfall variability. Artificial neural networks can adapt to nonlinear relationships, and this was evident with the prototype model. Once they were optimized for the chosen input variables, they were used to generate time series output that broadly matched rainfall at Kalamia (Fig. 3) and much better Pearson correlation coefficients (Table 2).

#### 4. Results

The simplest model for Kalamia had a single attribute as input, rainfall for the current month, with the target output being forecast rainfall with a 3-month lead. This forecast was then compared to the observed 3-month moving average (Pearson correlation coefficient = 0.60). Inclusion of the full set of lagged rainfall values gave an improved forecast (Pearson correlation coefficient = 0.64), and a time-series curve with sharper peaks and broader troughs (Fig. 3a). Marginal improvement was next achieved by

also inputting the atmospheric temperature dataset (Fig. 3b; Pearson correlation coefficient = 0.69; Table 2). Inputting the SOI also had limited impact, (Fig. 3c; Pearson correlation coefficient = 0.65). A more significant improvement came with the addition of the PDO (Pearson correlation coefficient = 0.75) by increasing the forecast rainfall for summers with observed higher rainfall (e.g., 1999 and especially 2009). The input of Niño 3.4 modulated this addition and improved the overall fit of forecast and observed rainfall (Fig. 3e). Inclusion of the solar attributes, solar irradiance, and sunspot number did not enhance performance of the model, and inclusion of the IOD did not improve it significantly (Table 2).

The best combination tested in this study (current and lagged rainfall, temperatures, SOI, PDO and Niño 3.4) reflected in the highest Pearson correlation coefficient and the lowest RMSE value (Table 2) was applied to the other high-quality rainfall sites in Queensland, and RMSE and Pearson correlation coefficients were calculated for each site (Table 3).

**Table 3.** Neural network forecast skill for Queensland high-quality rainfall sites. The error values, RMSEs, and Pearson correlation coefficients are used to compare the forecast monthly rainfall with 3-month lead compared to the 3-month observed moving average. The weighted non-dimensional index (WNDI) is used to normalize for differences in annual rainfall between sites.

Location	Pearson	RMSE (mm month <sup>-1</sup> )	Rainfall (mm yr <sup>-1</sup> )	WNDI
Auguthella	0.49	28.5	535.6	0.639
Ayrshire	0.61	30.5	403.2	0.908
Barcaldine	0.61	27.4	503.0	0.655
Burketown	0.66	80.9	784.0	1.238
Cheriton	0.49	25.3	549.3	0.553
Fairymead	0.56	41.9	1079.0	0.465
Harrisville	0.60	32.9	800.5	0.490
Isisford	0.58	26.3	454.5	0.695
Jandowae	0.64	23.6	664.1	0.427
Kalamia	0.71	66.3	1071.0	0.702
Macknade	0.77	110.5	2149.9	0.617
Miles	0.38	27.6	653.4	0.506
Palmerville	0.88	50.6	1051.2	0.573
Pittsworth	0.56	29.9	699.7	0.513
Pleystowe	0.76	77.7	1649.3	0.565
Surat	0.59	21.5	590.0	0.438
Townsville	0.72	82.9	1197.5	0.831
UQ Gatton	-0.58	34.1	771.6	0.533
Urandangie	0.60	26.8	301.2	1.070
Warrnambool	0.62	23.5	370.5	0.761

To compare the skill of the neural network among sites, the RMSE values were normalized by dividing the corresponding monthly average rainfall to give a weighted non-dimensional index (WNDI) after Johns et al. (2006) (Table 3).

It is not standard practice for climate scientists to provide RMSE values for output from their GCMs or output as time series graphs. Yet both of these methods allow easy comparisons across platforms and are arguably more transparent than the current reliance on colored maps and correlations (e.g., Hudson et al., 2011). Indeed a high linear correlation can be misleading if the set of predicted values is consistently a constant multiple of the target value. RMSE, in particular, gives a simple, transparent quantitative measure of the difference between what is forecast and/or calculated and what is observed and/or the target, and this measure is easily understood across disciplines.

WNDI values varied with Burketown, a site in northern central Queensland, reflecting the worst forecast skill with an RMSE of 1.238 and Jandowae, in southeast Queensland, reflecting the the best RMSE at 0.427. However, there were no obvious general differences in skill between inland and coastal locations or more northern versus southern locations (Fig. 1 and Table 3).

To facilitate a direct comparison between the forecasting skill of our neural network and the skill of the general circulation model POAMA-1.5, Oscar Alves

(Centre for Australian Weather and Climate Research, Australian Bureau of Meteorology) provided output from POAMA, including monthly average rainfall forecasts with a 3-month lead for 18 of our 20 high-quality rainfall sites. The values were provided as anomalies and simple bilinear interpolations of surrounding grid points; the interpolation was necessary for POAMA forecasts for 250-km<sup>2</sup> grid boxes. From these values, we calculated monthly rainfall then RMSE and WNDI values (Table 4). Time series plots of output for POAMA and also the neural network for five of the high quality rainfall sites are shown in Fig. 3. The forecast with a 3-month lead was compared with observed rainfall for the same month (Fig. 4).

Both models occasionally produced negative values for rainfall forecasts during the drier months. In all cases, negative values were adjusted to zero rainfall as a physical constraint on the system before RSME values were calculated.

The neural network is generally more skilled at forecasting rainfall 3 months in advance giving a lower RMSE compared to the RMSE for POAMA for each location, with the exception of Burketown (Table 4). The time series plots for Burketown are remarkably similar for the two very different models: neural network (Fig. 4e) versus GCM (Fig. 4f). Neither the neural network nor the POAMA forecast the observed peak in rainfall for Burketown of ~400 mm over the Australian summer of 1997–1998 (Figs. 4e and f). The



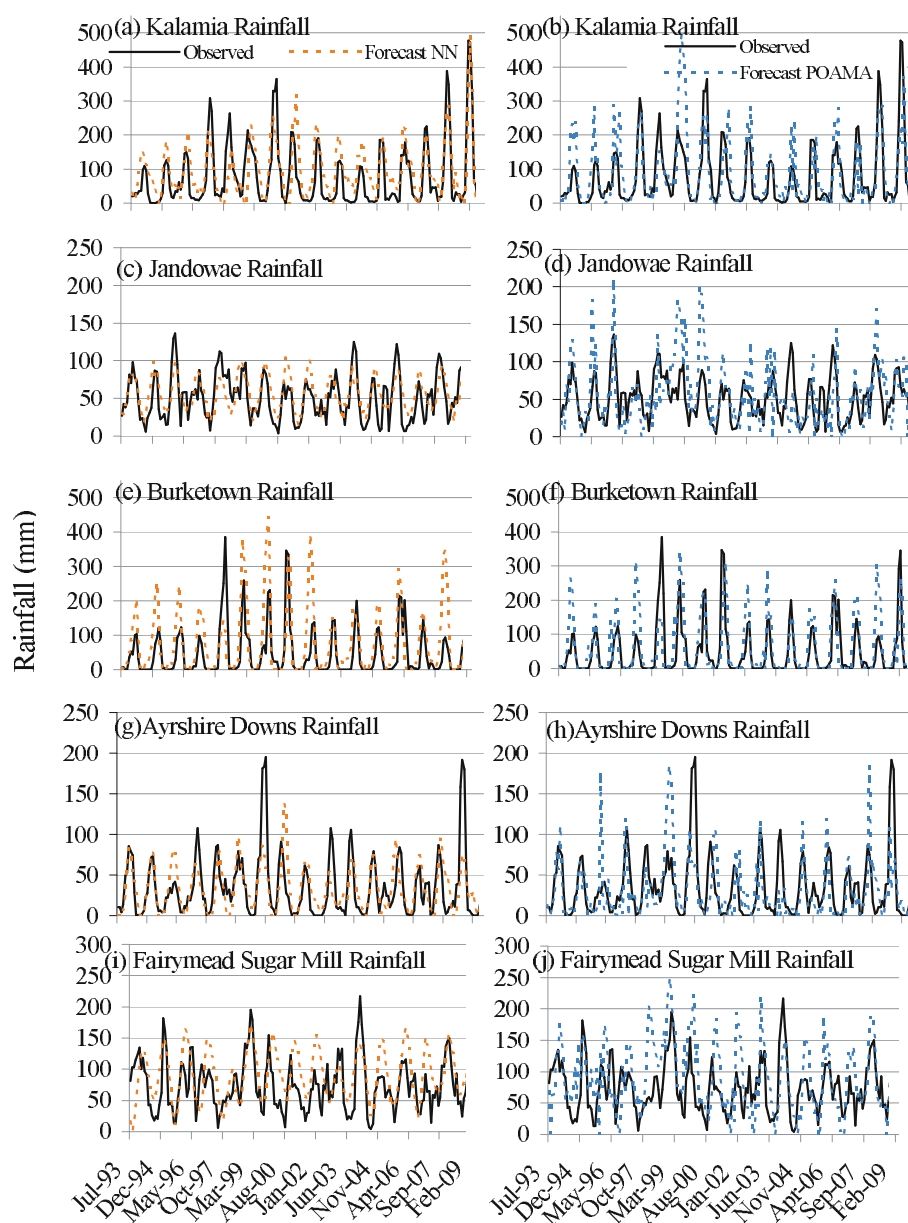


**Fig. 4.** Neural Network forecast versus POAMA forecast for five high-quality rainfall sites. Forecast rainfall (mm) is monthly with 3-month lead, compared to observed 3-month moving average.

neural network grossly overestimated rainfall values during the summer of 2001. Both the neural network and POAMA overestimated rainfall for the summer of 2007–2008.

At Kalamia the neural network and POAMA both underestimated rainfall for the Australian summers of 1996–1997 and 1999–2000 (Fig. 4a and b). POAMA grossly overestimated rainfall for the summer 1998–1999 and underestimated rainfall for the summer of 2008–2009 (Fig. 4b).

The neural network forecast the very wet summer of 2008–2009 at Kalamia (Fig. 4a), but it did not forecast this same event at Ayrshire Downs (Fig. 4g). POAMA did forecast three wet summers for Ayrshire Downs (Fig. 4h), and these events approximated the magnitude, but not timing, of the two exceptionally wet summers of 1999–2000 and 2008–2009 (Fig. 4h).

The POAMA forecasts for both Jandowae and Fairymead Sugar Mill (Figs. 4d and j), were much noisier than the corresponding forecasts by the neural

**Table 4.** Comparing forecast skill of POAMMA with the neural network (NN). RMSE is a comparison of the monthly forecast 3 months in advance with the observed rainfall for that month. WNDI is a normalized value to facilitate comparisons among locations with different rainfall amounts.

Location	RMSE NN (mm month <sup>-1</sup> )	RMSE POAMMA (mm month <sup>-1</sup> )	Rainfall (mm yr <sup>-1</sup> )	WNDI NN	WNDI POAMA
Augathella	46.6	51.8	535.6	1.044	1.161
Ayrshire	47.9	52.1	405	1.419	1.544
Barcaldine	43.8	58.1	503	1.045	1.386
Burketown	117.7	114	784	1.802	1.745
Cheriton	42.6	52.3	549.3	0.931	1.143
Fairymead	66.1	80.7	1079	0.735	0.897
Harrisville	49.4	64.7	820	0.723	0.947
Isisford	41	53.8	454.5	1.083	1.420
Jandowae	41.2	55.2	664.1	0.744	0.997
Kalamia	102.1	124.4	1071	1.144	1.394
Miles	44.9	57.4	653.4	0.825	1.054
Palmerville	80.7	88	1051.2	0.921	1.005
Pittsworth	47	59.8	699.7	0.806	1.026
Pleystowe	135.4	157.6	1649.3	0.985	1.147
Townsville	130.2	139.1	1197.5	1.305	1.394
UQ Gatton	53.6	64.5	777.6	0.827	0.995
Urandangie	44.4	47.1	301.2	1.769	1.876

network (Figs. 4c and i). While POAMA appeared to overestimate and underestimate seasonal rainfall at these sites over the period July 1993 to December 2009, the neural network underestimated particularly the drier periods (Figs. 4c and i). There may be an opportunity to significantly improve the skill of the neural network through the optimization processes by focusing on these drier periods. In particular, given the nature of the optimization process, the neural network model would apparently have more to gain in minimizing errors through focusing on wet months because they contain larger values, and they may thus preferentially influence the optimization process.

The Queensland Climate Change Centre of Excellence has developed a statistical model to forecast rainfall in Queensland's grazing lands for the 5-month period from November to March each year, a period it defines as summer. The Seasonal Pacific Ocean Temperature Analysis-1, SPOTA-1, uses its own climate indices based on differences in SST patterns in the Pacific Ocean. The most accurate SPOTA forecasts are made in any particular year at the start of November for the following 5-month summer period. The average lead-time for the SPOTA rainfall forecast is thus 2.5 months.

It was inherently more difficult to make a direct comparison between the neural network and the SPOTA 5-month seasonal forecast, than with POAMA. To compare output from our prototype with SPOTA, we calculated an average monthly rainfall for the 5-month summer period with a 3-month lead using

the forecast values previously described (Table 5).

Comparing the WNDI values of 0.410 for SPOTA to the WNDI value of 0.509 for the neural network indicates that SPOTA is more skilled at forecasting summer rainfall in Queensland's rangelands (Table 5). This could be because the indices used by SPOTA are superior, or the difference may be due to the smaller average lead-time used in this comparison for SPOTA (2.5 months), or it could be a function of differences in the geographic area or time periods that were compared.

Although the neural network model output for the 5-month period may appear less accurate than the SPOTA-1 forecast, it does contain additional information. The neural network output provides information on the distribution of rainfall within the 5-month period as well as the total amount of rainfall.

## 5. Discussion and conclusions

Australia has particularly variable rainfall patterns (Nicholls et al., 1997). During the past decade, eastern Australia has experienced persistent drought followed by catastrophic flooding, with three-quarters of the state of Queensland declared a natural disaster in January 2011 (Hurst, 2011).

The Australian Bureau of Meteorology has directed some of its research effort over this period towards the development of a GCM, the POAMA. This computer model of the climate system can provide a dynamic seasonal rainfall forecast, with most skill at predict-

**Table 5.** Comparison of forecast skill of SPOTA with the neural network for summer\* in the rangelands. The neural network WNDI scores are a comparison of observed average monthly rainfall for the period July 1993 to December 2009 for summer to the forecast average monthly rainfall with a 3-month lead. The SPOTA WNDI compares the observed average monthly rainfall for the period 1890–2010 for summer to the forecast average monthly rainfall with a lead time varying from 0 to 5 months.

Locations	RMSE (mm month <sup>-1</sup> )	Rainfall (mm yr <sup>-1</sup> )	WNDI
Neural Network Values			
Auguthella	20.6	535.6	0.461
Ayrshire	32.8	403.2	0.976
Barcaldine	20.7	503.0	0.493
Cheriton	21.2	549.3	0.464
Fairymead	38.6	1079.0	0.429
Harrisville	23.1	800.5	0.346
Isisford	19.9	454.5	0.526
Jandowae	14.4	664.1	0.260
Kalamia	55.9	1071.0	0.626
Macknade	106.0	2149.9	0.591
Miles	26.9	653.4	0.494
Pittsworth	22.5	699.7	0.385
Pleystowe	66.5	1649.3	0.484
Surat	16.2	590.0	0.330
Townsville	73.5	1197.5	0.74
UQ Gatton	26.7	771.6	0.423
Warrnambool	20.4	370.5	0.637
Average Neural Network Value			0.509
SPOTA Value			0.410

Note: \*Summer is defined by SPOTA as the months November, December, January, February, and March.

ing rainfall during austral winter and spring seasons increasing during dry period extremes of the ENSO (Hudson et al., 2011).

GCMs, including POAMA, are built up from an understanding of the physical processes that create weather. They are mathematical representations of general atmospheric circulation patterns based on the Navier–Stokes equations using thermodynamic terms to incorporate phase change and Earth’s energy budget. According to Zwiers and Von Storch (2004), improvements in forecasts by these models is likely to come from a better understanding of the dynamics of the system, but so far improvement has been limited by its complexity and by the many apparently non-linear relationships that do not yield to analysis from primary principles.

In Australia, the dynamic systems are often quantified and measured through climate indices. Roger Stone (Stone et al., 1996), Scott Power (Power et al., 2006), Stewart Franks (Kiem et al., 2003), Ken Day (2010) and others have emphasized the importance of these indices for rainfall forecasts in Queensland. Our understanding of these drivers of rainfall variability continues to improve (e.g., Risbey et al., 2009), but Vaze et al. (2011) claim that GCMs still fail to simu-

late actual observed annual rainfall time series or the trend in annual rainfall (Vaze et al., 2011). POAMA has, however, significant skill at forecasting some of the actual climate indices and the Bureau of Meteorology issues, for example, daily advice on the state of the ENSO based on forecasts from this GCM with this information then incorporated into statistical models.

In their review of the role of statistics in climate research, Zwiers and Von Storch (2004) explained how statistical analyses can help identify which pieces of information derived from observations of the climate system are worthy of synthesis and interpretation, but they are pessimistic specifically about the application of neural networks, in particular claiming that, while neural networks can substantially reduce the cost of the operational processing of high volumes of remotely sensed data, they have not improved our ability to synthesize knowledge.

We dispute this premature conclusion. Our prototype neural network for rainfall prediction in Queensland can improve the synthesis of knowledge and the actual seasonal forecast.

A problem for the many researchers who have used climate indices to forecast Queensland rainfall is that their models have thus far limited them to consider-

ing combinations of linear correlations individually. In contrast, our prototype neural network has the ability to consider large numbers of climate indices and other inputs simultaneously and to find solutions independently of assumed relationships.

In our first attempt at optimizing the neural network for a given set of input attributes, we found that patterns within rainfall data alone can provide a forecast (Fig. 3a). Our optimal model included current rainfall, lagged rainfall, atmospheric temperature, SOI, PDO, and Niño 3.4 as input attributes. The inclusion of PDO significantly improved the forecast of the magnitude of rainfall at Kalamia during the summer of 2008–2009, suggesting a role for this index, which has thus far been excluded from official Australian Bureau of Meteorology statistical forecasts.

RMSE values for our prototype neural network suggest its skill at forecasting rainfall with a 3-month lead at least as good as POAMA for Queensland's high-quality rainfall observation data (Table 4).

Time series output from POAMA and our prototype neural network (Fig. 3) indicate that both models can simulate the actual timing of annual rainfall time series (cf. Vaze et al., 2011, but they often fail to capture the magnitude of specific events. POAMA does appear to perform better at simulating drier periods (e.g., Burketown in Fig. 3f) and the neural network is more skilled at capturing the magnitude of some wet summers (e.g. Kalamia in Fig. 3a).

The impetus for the development of the prototype materialized only recently, after the flooding of Brisbane in January 2011. Output and design of the prototype is still considered experimental and preliminary. Design improvements may be made through focusing on drier periods, particularly during the optimization process. There is also significant potential for further experimentation with input variables, including the use of the potentially superior indices used by SPOTA. Furthermore, a neural network does allow for results from other techniques to be combined, so output from POAMA, in particular its forecast SOI index, could be input into our prototype, likely significantly improving forecast skill.

Although they are not developed from a first principles understanding of physical processes, further research into the application of artificial neural networks to rainfall forecasting in Queensland is likely to result in a significantly improved seasonal rainfall forecast, and this likelihood has an intrinsic real value.

**Acknowledgements.** This work was funded by the B. Macfie Family Foundation. We are grateful to Griff Young and Oscar Alves, of The Centre for Australian Weather and Climate Research, Bureau of Meteorology,

for data enabling direct comparison with output from the Neural Network. Oscar, Griff and also Ken Day, Queensland Climate Change Centre of Excellence, provided advice and insights.

## REFERENCES

- ASCE Task Committee on Application of Artificial Neural Networks in Hydrology, 2000a: Artificial neural networks in hydrology. I: Preliminary concepts. *J. Hydrol. Eng.*, **5**, 115–123.
- ASCE Task Committee on Application of Artificial Neural Networks in Hydrology, 2000b: Artificial neural networks in hydrology. II: Hydrological applications. *J. Hydrol. Eng.*, **5**, 124–137.
- Bilgili, M., and B. Sahin, 2010: Prediction of Long-term Monthly Temperature and Rainfall in Turkey. *Energy Sources*, **32**, 60–71.
- Braganza, K., J. L. Gergis, S. B. Power, J. S. Risbey, A. M. Fowler, 2009: A multiproxy index of the El Niño–Southern Oscillation, A. D. 1525–1982. *J. Geophys. Res.*, **114**, D05106.
- Castellani, L., I. Becchi, and F. Castelli, 1996: Rainfall Frequency and Seasonality Identification through Artificial Neural Networks. *Meccanica*, **31**, 117–127.
- Chakraverty, S., and P. Gupta. 2008: Comparison of neural network configurations in the long-range forecast of southwest monsoon rainfall over India. *Neural Computing & Applications*, **17**, 187–192.
- Chattopadhyay, S., and G. Chattopadhyay, 2008: Comparative study among different neural net learning algorithms applied to rainfall time series. *Meteorological Applications*, **15**, 273–280.
- Day, K. A., D. G. Ahrens, and A. Peacock, 2010: Seasonal Pacific Ocean Temperature Analysis-1 (SPOTA-1) as at November 1, 2010. Report issued by the Queensland Climate Change Centre of Excellence, Queensland Government, Brisbane, Australia, 2pp. [Available online from <http://www.longpaddock.qld.gov.au/spota1-getpassword.html>]
- Elman, J. L., 1990: Finding structure in time. *Cognitive Science*, **14**, 179–211.
- Erlykin, A. D., G. Gyalai, K. Kudela, T. Sloan, and A. W. Wolfendale, 2009: On the correlation between cosmic ray intensity and cloud cover. *Journal of Atmospheric and Solar-Terrestrial Physics*, **71**, 1794–1806.
- Firth, L., M. L. Hazleton, and E. P. Campbell, 2005: Predicting the Onset of Australian Winter Rainfall by Nonlinear Classification. *J. Climate*, **18**, 772–781.
- Freiwan, M., and H. K. Cigizoglu, 2005: Prediction of total monthly rainfall in Jordan using feed-forward back-propagation method. *Fresenius Environmental Bulletin*, **14**, 142–151.
- French, M. N., W. F. Krajewski, and R. R. Cuykendall, 1992: Rainfall forecasting in space and time using a neural network. *J. Hydrol.*, **137**, 1–31.
- Frohlich, C., 2000: Observations of irradiance variations. *Space Science Rev.*, **94**, 15–24.

- Giles, C. L., S. Lawrence, and A. C. Tsoi, 1997: Rule inference for financial prediction using recurrent neural networks. *Proc. IEEE/IAFE Conf. on Computational Intelligence for Financial Engineering*, IEEE Press, Piscataway, NJ, 253–259.
- Gholizadeh, M. H., and M. Darand, 2009: Forecasting Precipitation with Artificial Neural Networks (Case Study: Tehran). *J. Appl. Sci.*, **9**, 1786–1790.
- Guhathakurta, P., M. Rajeevan, and V. Thapliyal, 1999: Long range forecasting indian summer monsoon rainfall by a hybrid principal component neural network model. *Meteorology and Atmospheric Physics*, **71**, 255–266.
- Hartmann, H., S. Beckerb, and L. King. 2008: Predicting summer rainfall in the Yangtze River basin with neural networks. *Int. J. Climatol.* **28**, 925–936.
- Htike, K. K., and O. O. Khalifa, 2010: Rainfall forecasting models using focused time-delay neural networks. *Int. Conf. on Computer and Communication Engineering*, Kuala Lumpur, Malaysia, 1–6. [Available online at <http://dx.doi.org/10.1109/ICCCE.2010.5556806>]
- Hudson, D., O. Alves, H. H. Hendon, and A. G. Marshall, 2011: Bridging the gap between weather and seasonal forecasting: Intraseasonal forecasting for Australia. *Quart. J. Roy. Meteor. Soc.* **137**, 673–689.
- Hurst, D., 2011: Three-quarters of Queensland a disaster zone. Brisbane Times, Fairfax Media. [Available online at <http://www.brisbanetimes.com.au/environment/weather/threequarters-of-queensland-a-disaster-zone-20110111-19mf8.html>].
- Iseri, Y., G. C. Dandy, H. R. Maier, A. Kawamura, and K. Jinno, 2005: Medium term forecasting of rainfall using artificial neural Networks. *Modelling and Simulation Society of Australia and New Zealand*, A. Zerger and R. M. Argent, Eds., 1834–1840.
- Johns, T. C., and Coauthors, 2006: The New Hadley Centre Climate Model (HadGEM1): Evaluation of coupled simulations. *J. Climate*, **19**, 1327–1353.
- Karamouz, M., S. Razavi, and S. Araghinejad, 2008: Long-lead seasonal rainfall forecasting using time-delay recurrent neural networks: A case study. *Hydrological Processes*, **22**, 229–241.
- Kiem, A., S. Franks, and G. Kuczera, 2003: Multi-decadal variability of flood risk. *Geophys. Res. Lett.*, **30**(2), 1–7.
- Kirkby, J., and Coauthors, 2011: Role of sulphuric acid, ammonia and galactic cosmic rays in atmospheric aerosol nucleation. *Nature*, **476** (7361), 429–435.
- Kirono, D. G. C, F. H. S. Chiew, and D. M. Kent 2010: Identification of best predictors for forecasting seasonal rainfall and runoff in Australia. *Hydrological Processes*, **24**, 1237–1247.
- Kulshretha, M. S., and R. K. George, 2007: Prediction of annual rainfall by double Fourier series and artificial neural network. *Neural, Parallel & Scientific Computations*, **15**, 539–546.
- Laken, B. A., D. R. Kniveton, and M. R. Frogley, 2010: Cosmic rays linked to rapid mid-latitude cloud changes. *Atmos. Chem. Phys.*, **10**, 10941–10948.
- Long, J., L. Ying, and L. Zhenshan, 1997: Comparison of long-term forecasting of June–August Rainfall over Changjiang–Huaihe Valley. *Adv. Atmos. Sci.*, **14**, 87–92.
- Luk, K. C., J. E. Ball, and A. Sharma, 2000: A study of optimal model lag and spatial inputs to artificial neural network for rainfall forecasting. *J. Hydrol.*, **227**, 56–65.
- Luk, K. C., J. E. Ball, and A. Sharma, 2001: An application of artificial neural networks for rainfall forecasting. *Mathematical and Computer Modelling.*, **33**, 883–699.
- Marshal, A. G., D. Hudson, M. C. Wheeler, H. H. Hendon, and O. Alves, 2011: Simulation and prediction of the Southern Annular Mode and its influence on Australian intra-season climate in POAMA. *Climate Dyn.* (in press)
- McBride, J. L., and N. Nicholls, 1983: Seasonal relationships between Australian rainfall and the Southern Oscillation. *Mon. Wea. Rev.*, **111**, 1998–2004.
- Meinke, H., and R. Stone, 2005: Seasonal and inter-annual climate forecasting: the new tool for increasing preparedness to climate variability and change in agricultural planning and operations. *Climate Change.*, **70**, 221–253.
- Micevski, T., S. Franks, and G. Kuczera, 2006: Multi-decadal variability in coastal eastern Australian flood data. *J. Hydrol.*, **327**(1–2), 219–225.
- Michaelides, S. C., C. S. Pattichis, and G. Kleovoulou, 2001: Classification of rainfall variability by using artificial neural networks. *Int. J. Climatology*, **21**, 1401–1414.
- Mozer, M. C., and P. Smolensky, 1989: Skeletonization: a technique for trimming the fat from a network via relevance assessment. *Advances in Neural Information Processing Systems 1*, D. Touretzky, ED., Morgan Kaufmann, San Monteo, California, 107–115.
- Nasseri, M., K. Asghari, and M. J. Abedini, 2008: Optimized scenario for rainfall forecasting using genetic algorithm coupled with artificial neural network. *Expert Systems With Applications*, **35**, 1415–1421.
- Navone, H. D., and H. A. Ceccatto, 1994: Predicting Indian monsoon rainfall: A neural network approach. *Climate Dyn.*, **10**, 305–312.
- Nicholls, N., B. Lavery, C. Fredericksen, W. Drosowsky, and S. Torok, 1996: Recent apparent changes in relationships between the El Nino–southern oscillation and Australian rainfall and temperature. *Geophys. Res. Lett.*, **23**, 3357–3360.
- Nicholls, N., W. Drosowsky, and B. Lavery, 1997: Australian rainfall variability and change. *Weather*, **52**, 66–71.
- Philip, N. S., and K. B. Joseph, 2003: A neural network tool for analysing trends in rainfall. *Comput. Geosc.*, **29**, 215–223.
- Pineda, F. J., 1989: Recurrent back-propagation and the dynamical approach to adaptive neural computation. *Neural Computation*, **1**, 161–172.

- Power, S., T. Casey, C. Folland, A. Colman, and V. Mehta, 1999: Interdecadal modulation of the impact of ENSO on Australia. *Clim. Dynam.*, **15**, 319–324.
- Power, S. B., M. Haylock, R. Colman, and X. Wang, 2006: The Predictability of Interdecadal Changes in ENSO Activity and ENSO Teleconnections. *J. Climate*, **19**, 4755–4771.
- Queensland Flood Commission of Inquiry, 2011: Queensland Floods Commission of Inquiry: Interim Report, 1180pp. Brisbane, Queensland, Australia. [Available online from [www.floodcommission.qld.gov.au](http://www.floodcommission.qld.gov.au)]
- Rashid, H. A., H. H. Hendon, M. C. Wheeler, and O. Alves, 2011: Prediction of the Madden-Julian oscillation with the POAMA dynamical prediction system. *Climate Dyn.*, **36**(3), 649–661.
- Risbey, J. S., M. J. Pook, and P. C. McIntosh, 2009: On the remote drivers of rainfall variability in Australia. *Mon. Wea. Rev.*, **137**, 3233–3253.
- Seqwater. 2011: Report on the operation of Somerset Dam and Wivenhoe Dam: January 2011 Flood Event. Queensland Government, Brisbane, Australia.
- Silverman, D., and J. A. Dracup, 2000: Artificial neural networks and long-range precipitation prediction in California. *J. Appl. Meteor.*, **39**, 57–66.
- Stone, R. C., G. L. Hammer, and T. Marcussen, 1996: Prediction of global rainfall probabilities using phases of the southern oscillation index. *Nature*, **384**, 252–255.
- Suppiah, R., 2004: Trends in the southern oscillation phenomenon and Australian rainfall and changes in their relationship. *Int. J. Climatol.*, **24**, 269–290.
- Tangang, F. T., B. Tang, A. H. Monahan, and W. W. Hsieh, 1998: Forecasting ENSO Events: A neural network–extended EOF approach. *J. Climate*, **11**, 29–41.
- Thresher, R. E., 2002: Solar correlates of Southern Hemisphere mid-latitude climate variability. *Int. J. Climatol.*, **22**, 901–915.
- Tomasino, M., D. Zanchettin, and P. Traverso, 2004: Long-range forecasts of River Po discharges based on predictable solar activity and a fuzzy neural network model. *Hydrological Sciences Journal*, **49**, 673–684.
- Ummenhofer, C. C., M. H. England, P. C. McIntosh, G. A. Meyers, Michael J. Pook, J. S. Risbey, A. Sen Gupta, and A. S. Taschetto, 2009: What causes southeast Australia's worst droughts? *Geophys. Res. Lett.*, **36**, L04706.
- Vaze, J., J. Teng, and F. H. S. Chiew, 2011: Assessment of GCM simulations of annual and seasonal rainfall and daily rainfall distribution across south-east Australia. *Hydrological Processes*, **25**, 1486–1497.
- Venkatesan, C., S. D. Raskar, S. S. Tambe, B. D. Kulkarni, and R. N. Keshavamurty, 1997: Prediction of all India summer monsoon rainfall using error back propagation neural networks. *Meteorol. Atmos. Physics*, **62**, 225–240.
- Verdon, D. C., and S. W. Franks, 2006: Long-term behaviour of ENSO: Interactions with the PDO over the past 400 years inferred from paleoclimate records. *Geophys. Res. Lett.*, **33**(6), L06712.
- Versteegh, G. J. M., 2005: Solar forcing of climate. 2: Evidence from the past. *Space Science Reviews.*, **120**, 243–286.
- Vines, R. G., 2008: Australian rainfall patterns and the southern oscillation. 2. A regional perspective in relation to Luni-solar (Mn) and Solar-cycles (Sc) signals. *Rangeland Journal*, **30**, 349–359.
- Wang, Z., and H. Sheng, 2010: Rainfall Prediction Using Generalized Regression Neural Network: Case study Zhengzhou. *Int. Conf. on Computational and Information Sciences*, Chengdu, Sichuan, China, 1265–1268.
- Wu, X., H. Cao, A. Flitman, F. Wei, and G. Feng, 2001: Forecasting monsoon precipitation using artificial neural networks. *Adv. Atmos. Sci.*, **18**, 950–958.
- Zhao, M., and H. H. Hendon, 2009: Representation and prediction of the Indian Ocean dipole in the POAMA seasonal forecast model. *Quart. J. Roy. Meteor. Soc.* **135**, 337–352.
- Zwiers, F. W., and H. Von Storch, 2004: On the role of statistics in climate research. *Int. J. Climatol.*, **24**, 665–680.